

Research Article

NAV-003, a bispecific antibody targeting a unique mesothelin epitope and CD3 ϵ with improved cytotoxicity against humoral immunosuppressed tumors

Luigi Grasso¹, Qun Jiang², Raffit Hassan², Nicholas C. Nicolaides¹
and J. Bradford Kline¹

¹ Navrogen Inc., Cheyney, PA, USA

² Thoracic and GI Malignancies Branch, CCR, NCI, NIH, Bethesda, MA, USA

Mesothelin (MSLN) is a cell surface protein overexpressed in a number of cancer types. Several antibody- and cellular-based MSLN targeting agents have been tested in clinical trials where their therapeutic efficacy has been moderate at best. Previous studies using antibody and Chimeric Antigen Receptor-T cells (CAR-T) strategies have shown the importance of particular MSLN epitopes for optimal therapeutic response, while other studies have found that certain MSLN-positive tumors can produce proteins that can bind to subsets of IgG1-type antibodies and suppress their immune effector activities. In an attempt to develop an improved anti-MSLN targeting agent, we engineered a humanized divalent anti-MSLN/anti-CD3 ϵ bispecific antibody that avoids suppressive factors, can target a MSLN epitope proximal to the tumor cell surface, and is capable of effectively binding, activating, and redirecting T cells to the surface of MSLN-positive tumor cells. NAV-003 has shown significantly improved tumor cell killing against lines producing immunosuppressive proteins *in vitro* and *in vivo*. Moreover, NAV-003 demonstrated good tolerability in mice and efficacy against patient-derived mesothelioma xenografts co-engrafted with human peripheral blood mononuclear cells. Together these data support the potential for NAV-003 clinical development and human proof-of-concept studies in patients with MSLN-expressing cancers.

Keywords: bispecific · CA125 · immunosuppression · mesothelin · NAV-003



Additional supporting information may be found online in the Supporting Information section at the end of the article.

Introduction

Mesothelin (MSLN) is a cell surface protein overexpressed on a number of cancer types and is actively being pursued clinically in antibody-based and cell-based therapeutic strategies [1].

While the function of MSLN is not completely understood, one defined role has been its involvement in heterotypic cellular adhesion where it has been found to bind the MUC16/CA125 protein on neighboring cells for cellular homeostasis and migration [2, 3]. While several anti-MSLN-targeted approaches are being pursued to treat MSLN-positive cancers [4], a new focus has been the development of antibodies that are refractory to immunosuppressive tumor produced proteins, referred to as humoral immuno-oncology (HIO) factors, which can suppress immune

Correspondence: Dr. Luigi Grasso
e-mail: luigi@navrogen.com

effector activities, or antibodies that can target epitopes optimal for cytotoxic immune effector activity [5, 6]. Previous studies have found that HIO factors such as MUC16/CA125 can bind to subsets of IgG1 antibodies and suppress their immune effector activities, including antibody-dependent cellular cytotoxicity (ADCC) and/or complement-dependent cytotoxicity (CDC) via blockade of CD16a Fc-gamma receptor and C1q protein IgG1 Fc binding, respectively [5–7]. Recently, we have discovered a new HIO factor, HIO-3, that binds to the CH3 domain of IgG1-type antibodies and suppresses the immune effector activity of tumor-targeting antibodies by reducing antibody-CD16a and antibody-C1q binding. This discovery emphasizes the need for antibody-based therapies that can be refractory to HIO factors immunosuppressive effects [8]. Recently, Tomar et al. compared the activity of two MSLN targeting antibodies in CAR-T format, called SS1 and YP218, which target the MSLN N-terminal region I and C-terminal region III that is proximal to the cell membrane, respectively [9–11]. In particular, the SS1 construct epitope overlaps with the MUC16/CA125 binding domain while the YP218 epitope is distal to this domain. The investigators demonstrated that the SS1 CAR-T was less effective than the YP218 construct potentially due to competition between SS1 and MUC16/CA125 binding the same MSLN region I. This competitive binding limits SS1 binding and killing of target cells and/or optimal positioning of the lymphocyte to the tumor cell surface for maximal cytotoxicity. In light of these limitations, anti-MSLN antibodies that target regions outside the MUC16/CA125 binding domain as well as proximal to the tumor cell surface and are engineered in alternative antibody-based formats (i.e., antibody drug conjugates, CAR-T, bispecific antibodies, etc.) may enable the development of more resilient agents refractory to the immunosuppressive effects of HIO factors.

Bispecific antibody formats potentially offer the ability to circumvent immunosuppression of HIO factors on antibody immune effector activities by juxtaposing activated cytotoxic lymphocytes or myeloid cells to the cell surface of a targeted tumor cell. This modality avoids the need for CD16a Fc-gamma receptor binding and subsequent activation of NK and macrophage effector cells or the binding of C1q protein to initiate the complement cascade, two initiating mechanisms that are required for humoral immune responses. In an attempt to develop more potent anti-MSLN targeting agents, we engineered the MSLN region III targeting humanized YP218 antibody (huYP218) into a full-length IgG1 bispecific format using a humanized single-chain anti-CD3 ϵ antibody fragment that is genetically fused to the N-terminal light chain of the huYP218, referred herein as NAV-003. We then tested NAV-003 activity against tumor cell lines producing immunosuppressive HIO factors *in vitro* and *in vivo*.

Here, we show that NAV-003 is able to retain strong MSLN and CD3 ϵ binding, activate primary T-cells *in vitro*, and effectively kill MSLN-positive tumor cells in the presence of endogenously produced and/or exogenously added HIO factors *in vitro* and *in vivo*. These findings suggest the engineering of HIO-refractory antibodies in bispecific format such as NAV-003 may improve therapeutic

efficacy and warrant its advancement to human clinical trials as a monotherapy to treat MSLN-positive cancers.

Results

Designing anti-MSLN/CD3 ϵ bispecific antibodies

Generation of bispecific antibodies that can specifically bind cell surface tumor antigens as well as bind and activate cell surface receptors on immune cells when juxtaposed to the tumor cell membrane requires optimal *cis*- or *trans*-configurations and spacing of the two antibody variable domains [12]. As non-Fc containing bispecific antibodies have limitations due to short serum half-lives [13], we chose to engineer NAV-003 as a humanized full-length IgG1 fused to a single-chain antibody. This format consists of the divalent anti-MSLN and anti-CD3 ϵ in a *cis*-configuration in which both binding domains are adjacent to each other. This configuration has been shown to yield better bispecific potency than *trans*-configured formats [12]. For the anti-MSLN component of NAV-003, we selected the humanized anti-MSLN YP218 antibody (huYP218) because it binds to a unique epitope in the MSLN region III [10], which is closest to the cell surface (Fig. 1A), while the single-chain anti-CD3 ϵ component was derived from the OKT3 antibody by humanization of its variable domains. Spatial orientation of the two binding components has also been shown to be important [12]. We have previously tested various configurations where the anti-CD3 ϵ single-chain antibody (scFv) on the N-terminal domain of the full-length IgG1 is fused either to the heavy or light chain, as well as explored using variable GGGG(x) linker repeats. In this preliminary screen (data not shown), the configuration of the anti-CD3 ϵ single-chain fused to the N-terminal domain of the huYP218 light chain via a single linker repeat was selected and further analyzed. NAV-003's schematic structure is shown in Fig. 1B, highlighting the *cis*-configured antigen binding domain regions for each antibody.

Binding analysis shows that the selected configuration for NAV-003 has robust MSLN and CD3 ϵ binding using purified recombinant antigens (Fig. 1C). To test for CD3 binding on T cells, parental Jurkat cells were incubated with NAV-003 or the parent anti-CD3 ϵ huOKT3 antibody and assayed for specific cell surface binding by immunofluorescence and comparing percent positive stained cells to the total cell count. NAV-003 specifically bound to CD3⁺/MSLN⁻ Jurkat cells to a level similar to the parent anti-CD3 ϵ huOKT3 antibody and the binding appears to be mediated by the anti-CD3 ϵ component as the parent anti-MSLN antibody, huYP218, did not bind Jurkat cells (Fig. 1D). Previous studies have shown that an affinity gap of 10-fold between the tumor targeting and the T-cell engaging antibodies allows the bispecific antibody to bind tumor first, therefore reducing the potential for immune receptor cross-linking, systemic T-cell activation, and cytokine release syndrome [14]. Employing surface plasmon resonance (SPR) analysis, we determined that the affinities of NAV-003's anti-MSLN and anti-CD3 ϵ components were 5 and 42 nM, respectively, representing an 8.4-fold higher

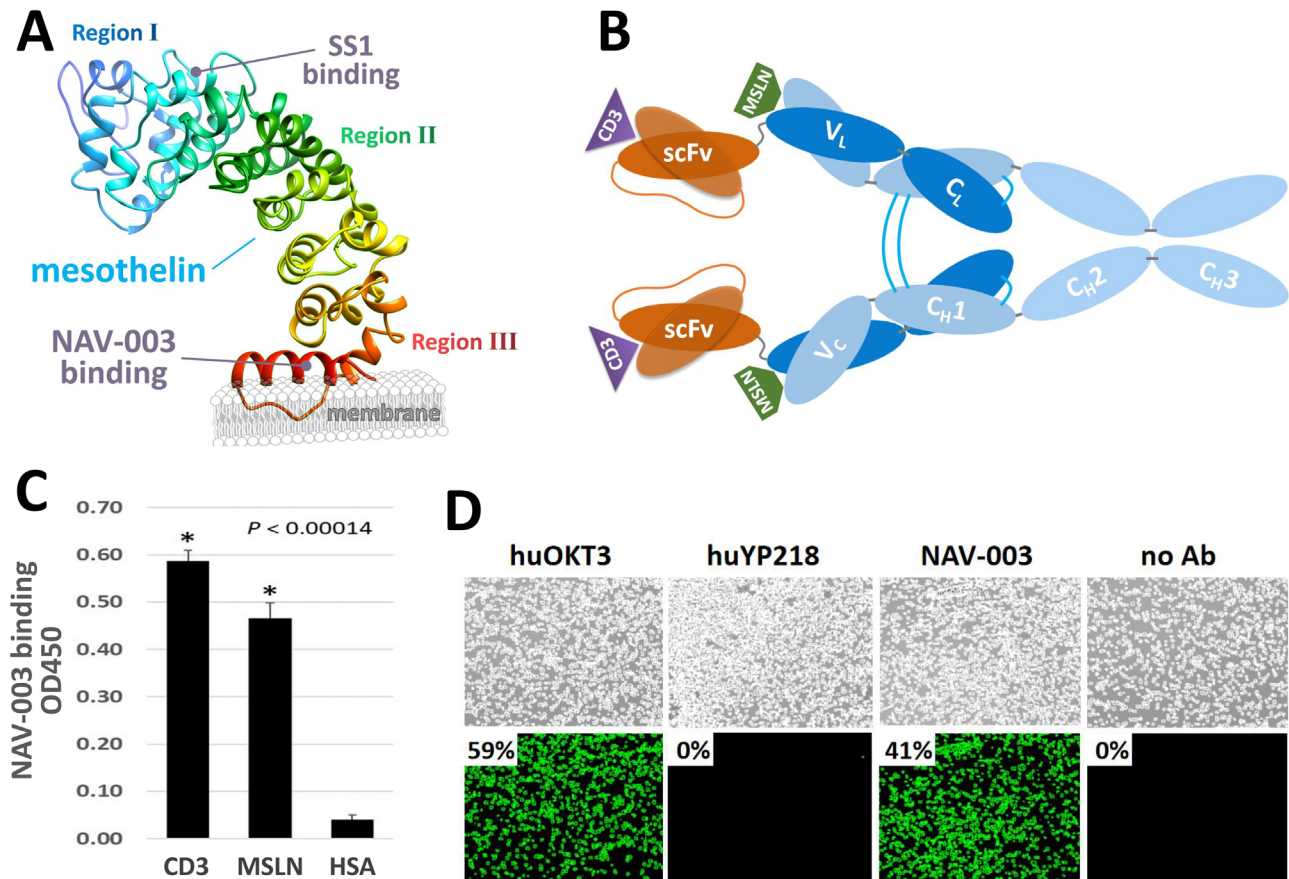


Figure 1. Construction and analysis of NAV-003. (A) 3D structure modeling of human MSLN where regions I, II, and III are indicated. NAV-003 binds to a unique epitope (amino acids 525–560) in region III, which is closest to the cell membrane, whereas SS1 binds to region I. (B) Schematic of NAV-003 bispecific configuration. (C) NAV-003 was tested via ELISA for binding to immobilized recombinant MSLN and CD3_ε proteins. Human serum albumin (HSA) was used as negative control. NAV-003 was able to bind both immobilized target antigens. Mean values are shown with error bars representing the standard deviations of sample replica. All statistics were calculated using the unpaired Student's *t*-test (two-tailed) and the *p* value is shown within the graph. (D) To evaluate NAV-003 engagement with CD3_ε on T-cells, an Alexa488-tagged secondary antibody was used to detect NAV-003, huYP218, and huOKT3 binding to Jurkat T-cells. NAV-003, via its anti-CD3_ε single-chain arm, bound to CD3_ε on CD3⁺/MSLN⁻ Jurkat cells at levels similar to the parent humanized OKT3 antibody. The percent of CD3⁺ positive cells detected by the various antibodies is indicated in the insets. A representative experiment of three independent experiments is shown.

affinity for MSLN versus CD3_ε (Supporting information Fig. S1A and B), thus approximating the desired affinity gap. In addition, SPR analysis confirmed that NAV-003, after binding MSLN, can then co-bind CD3_ε (Supporting information Fig. S1C), recreating the binding sequence scenario *in vivo* where tumor cells are bound first, due to higher affinity, and T cells are recruited next.

T-cell activation and target cell killing modalities mediated by NAV-003

The full-length IgG1 configuration of NAV-003 potentially enables the antibody to target MSLN tumors and kill via humoral immune effector activity such as ADCC through CD16a Fc-γ receptor activation as well as CD3-redirection, T-cell-mediated cytotoxicity. To evaluate the activity of NAV-003 using these cytotoxic mechanisms, two assays were employed. For CD16a activation, the engineered Jurkat CD16a-luciferase ADCC reporter assay was

employed along with the human MSLN-expressing Chinese Hamster Ovary cell line (CHO-MSLN) as the target cells.

As shown in Fig. 2A, NAV-003 was able to activate Jurkat CD16a receptor signaling via MSLN binding similarly as the parent huYP218 antibody, and this activation is dependent on the expression of MSLN since parent MSLN-negative CHO cells did not elicit this response. To compare the overall cytotoxic activity of NAV-003 to huYP218, human peripheral blood mononuclear cells (PBMCs) were employed to analyze their cytotoxicity against CHO-MSLN cells. As shown in Fig. 2B, while both NAV-003 and huYP218 had cytotoxic activity against CHO-MSLN as compared to no antibody, the NAV-003 cytotoxicity was significantly higher than huYP218 (EC_{50} 0.1 μg/mL vs. >10 μg/mL, *p* < 0.00025). These results suggest that the combination of ADCC and CD3-redirection, T-cell-mediated cytotoxicity was more robust than CD16a Fc-γ receptor mediated ADCC alone, the latter of which is the sole mechanism by which huYP218 can mediate cytotoxicity against target cells. As NAV-003 was confirmed to

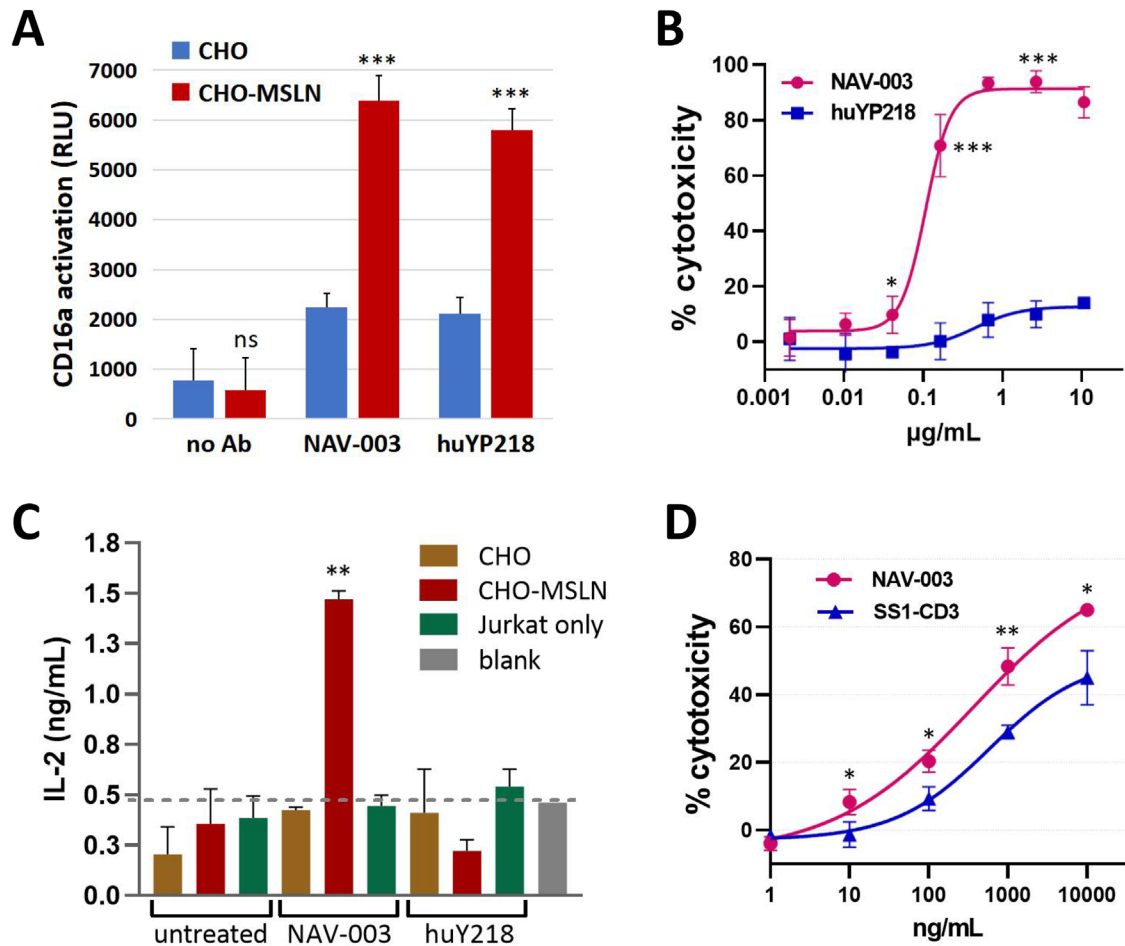


Figure 2. NAV-003-mediated killing of MSLN target cells via ADCC and cytotoxic T-cell activation. (A) CHO-MSLN cells or parent CHO cells were co-cultured with Jurkat-CD16a-luciferase reporter cells and treated with no antibody (no Ab), NAV-003, or huYP218 antibody. NAV-003 was able to activate CD16a Fc- γ receptor signaling at levels similar as the parent antibody, huYP218. (B) ADCC assay using CHO-MSLN as target cells and human PBMCs as effector cells. NAV-003 mediates superior cytotoxicity compared to huYP218. (C) Quantification of 24-h IL-2 production by Jurkat T cells. One-way ANOVA multiple comparison analysis shows that the only statistically significant IL-2 production by T cells was detected with NAV-003 treatment of CHO-MSLN cells but not with parent CHO cells or no target cells (Jurkat only). The IL-2 levels produced during the 24-h incubation were approximately 1.5 ng/mL. (D) NAV-003 has a statistically significant greater cytotoxicity (IC_{50} 365 ng/mL) against CA125-positive OVCAR3 cells compared to SS1-CD3 (IC_{50} 587 ng/mL). Representative experiments of three independent experiments are shown. IC_{50} s were calculated by the log(inhibitor) versus response curve fitting in Prism 9.5. Mean values are shown with error bars representing the standard deviations or SEM of sample replica. All statistics were calculated using the unpaired Student's t-test (two-tailed) or one-way ANOVA (panel C); * p value < 0.05; ** p value < 0.01; *** p value < 0.001; ns, statistically non-significant.

bind cell surface CD3 ϵ on parental Jurkat cells (Fig. 1D), we next assayed for the ability of NAV-003 to activate Jurkat T-cells alone or in the presence of MSLN-positive target cells. Co-cultures containing Jurkat cells plus either CHO cells, CHO-MSLN, or no target cells were treated with NAV-003, huYP218, or left untreated, and then analyzed for T-cell activation via IL-2 production. NAV-003 stimulated production of IL-2 through its interaction with CD3 as part of the T-cell receptor signaling cascade (Fig. 2C). Moreover, the NAV-003 T-cell activation appeared to require MSLN binding as no NAV-003-mediated IL-2 production was observed in cultures containing CHO cells or no target cells. In contrast, huYP218 antibody was unable to stimulate IL-2 production (Fig. 2C) as it can only engage with effector cells through its Fc domain while Jurkat cells lack Fc receptor expression.

As the SS1-based CAR-T was reported to be less effective than the huYP218-based construct potentially due to competition between SS1 and MUC16/CA125 binding the same MSLN region I [9, 10] (Fig. 1A), we compared the SS1-based MSLN/CD3 bispecific (SS1-CD3) to NAV-003 by testing their cytotoxicity against the MUC16/CA125-positive OVCAR3 cells (see MUC16/CA125 expression analysis in Supporting information Fig. S2). NAV-003 showed a statistically significant greater cytotoxicity compared to SS1-CD3 (Fig. 2D), thus suggesting the beneficial effects of binding to MSLN's region III, which is closest to the cell membrane and away from the MSLN/CA125 binding site (region I).

Studies have reported on the effect of Fc-mediated functions on a bispecific antibody as they relate to either its ADCC/CDC activity or pharmacokinetic profiles [15]. To assess the impact of

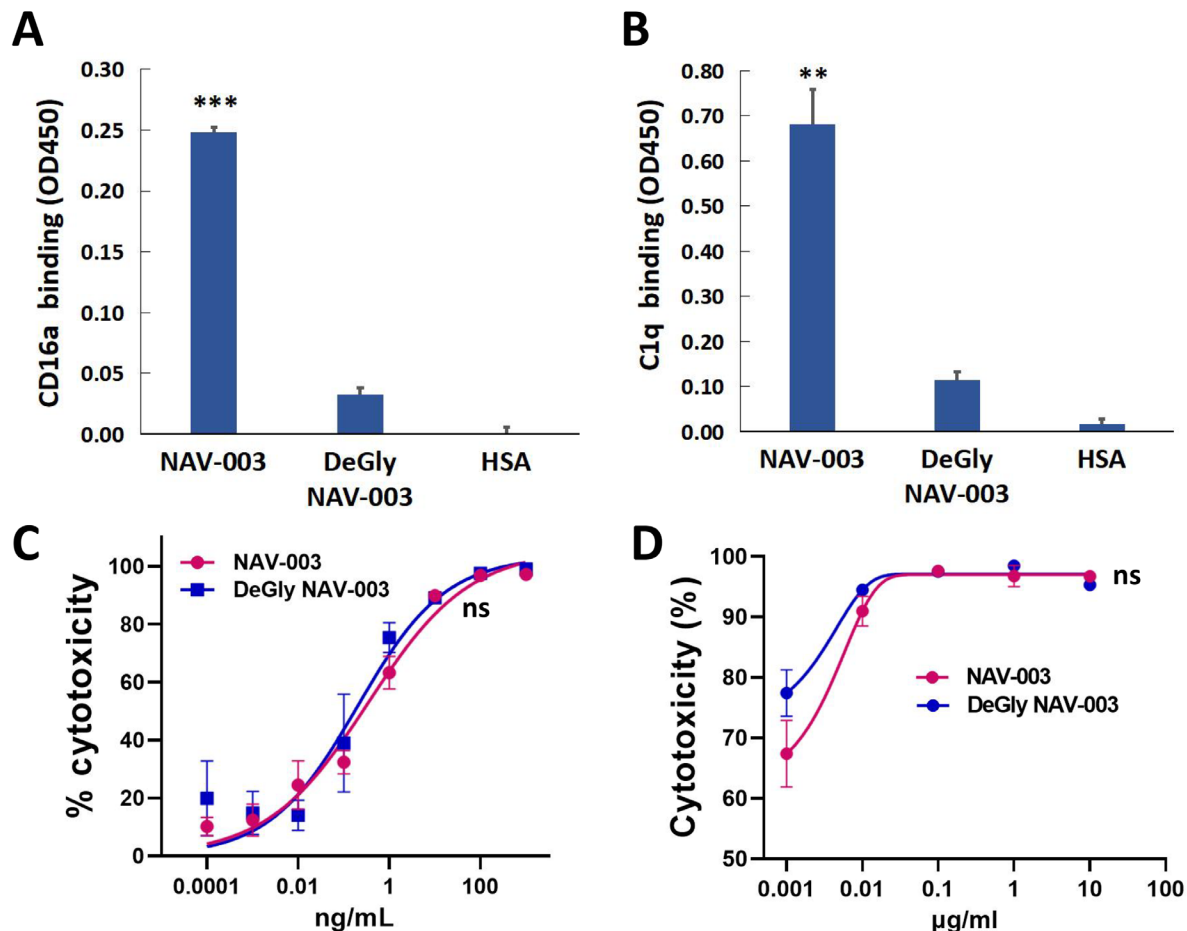


Figure 3. Deglycosylation of NAV-003 leads to loss of CD16a and C1q binding but no change in cytotoxicity activity in vitro. Removal of glycosyl groups significantly reduced the binding of deglycosylated NAV-003 (DeGly NAV-003) to CD16a Fc- γ receptor (A) and C1q (B) compared to native NAV-003. Loss of Fc-mediated function did not appear to have any significant impact on NAV-003-mediated killing *in vitro* against OVCAR3 cells (C) or NCI-Meso63 tumor cells (D), as the EC_{50} of native NAV-003 and DeGly NAV-003 were comparable (0.34 and 0.20 ng/mL, respectively, in OVCAR3, and 0.95 and 0.96 ng/mL, respectively, in NCI-Meso63). The data suggest that the cytotoxicity mediated through the Fc- γ receptor is negligible when compared to the CD3-redirected, T-cell-mediated cytotoxicity. A representative experiment of three independent experiments is shown. IC_{50} s were calculated by the log(inhibitor) versus response curve fitting in Prism 9.5. Mean values are shown with error bars representing the standard deviations or SEM of sample replica. All statistics were calculated using the unpaired Student's *t*-test (two-tailed). **p* value < 0.05; ***p* value < 0.01; ****p* value < 0.001; ns, statistically non-significant.

removing the Fc-mediated function, NAV-003 was deglycosylated as described in Materials and methods section to generate DeGly NAV-003. As expected, deglycosylation resulted in loss of NAV-003 binding to CD16a Fc- γ receptor (Fig. 3A) and C1q protein (Fig. 3B) confirming removal of the Fc-mediated function when compared to native NAV-003. Next, NAV-003 and DeGly NAV-003 were compared by using a cytotoxicity assay employing PBMCs and OVCAR3 target cells. As shown in Fig. 3C, deglycosylation did not appear to have any significant impact on NAV-003-mediated killing ($p \geq 0.79$), with EC_{50} of native NAV-003 and DeGly NAV-003 being comparable (0.34 and 0.20 ng/mL, respectively). Similar results were obtained when using different tumor cells (NCI-Meso63) and batches of human PBMCs (Fig. 3D). Because loss of Fc-receptor binding did not affect NAV-003 cytotoxicity under the conditions tested, these data suggest that the cytotoxicity component mediated through the Fc- γ receptor is less prominent when

compared to the CD3-redirected, T-cell-mediated cytotoxicity, as also predicted by the comparison between huYP218, which cannot bind to CD3, and NAV-003 (Fig. 2B). Both deglycosylated and native NAV-003 were later tested *in vivo* to assess efficacy as well as any pharmacokinetic changes that may impact these two versions.

NAV-003 activity against humoral immunosuppressive tumor cells and tumor-produced HIO factors

Several reports have shown that tumor-produced HIO factors can have significant immunosuppressive effects on antibody-mediated tumor cell killing [16, 17]. This has been highlighted by studies monitoring the effects of HIO factors such as MUC16/CA125 and

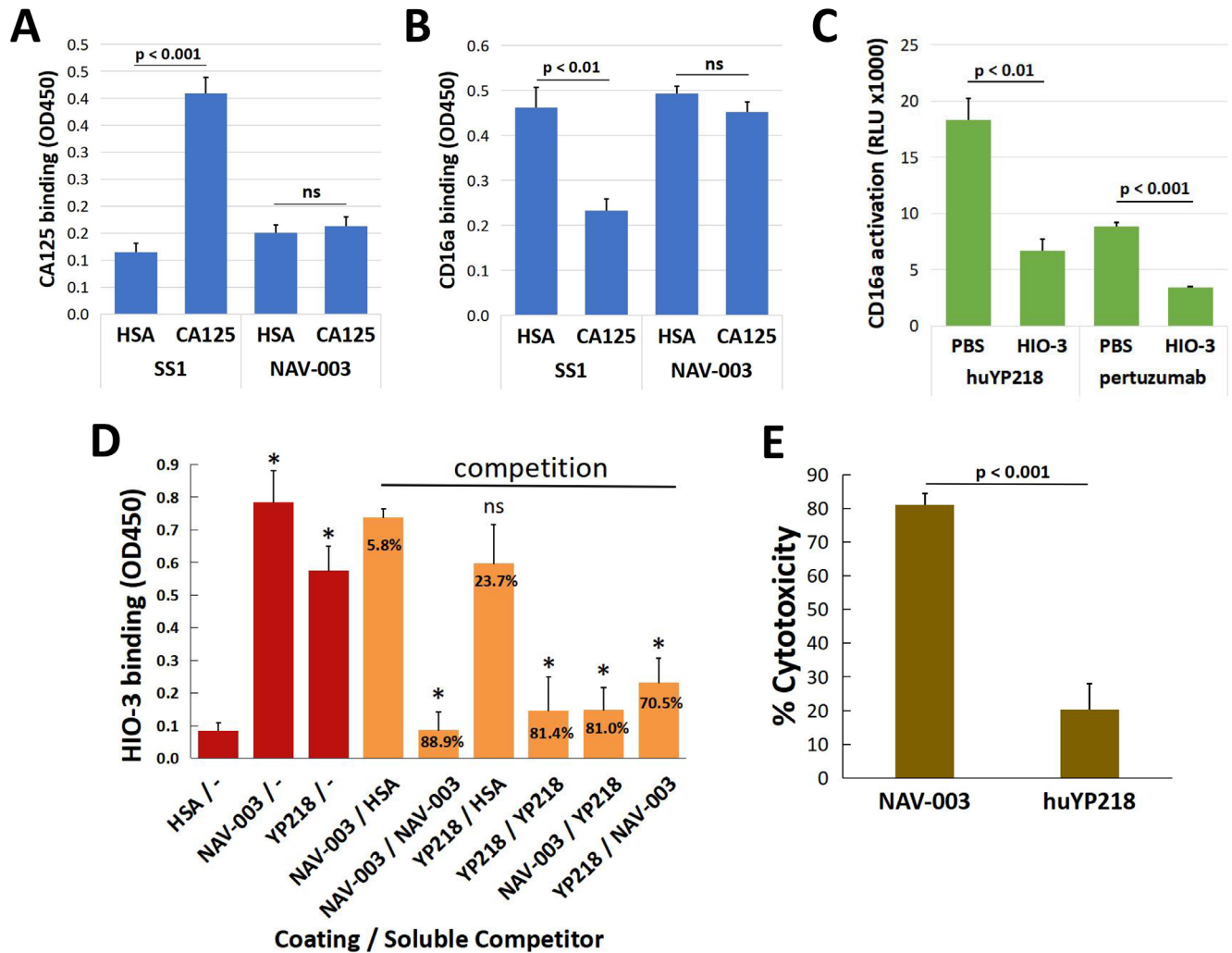


Figure 4. NAV-003 is active in the presence of immunosuppressive HIO factors. Immunosuppressive HIO factors such as MUC16/CA125 or HIO-3 can suppress the therapeutic activity of antibody-based agents by direct binding and suppression of ADCC due to reduced CD16a/antibody binding. NAV-003 is refractory to MUC16/CA125 binding (A) and shows unaltered CD16a engagement in the presence of MUC16/CA125 (B), in contrast to the MUC16/CA125-sensitive SS1 antibody. (C) The immunosuppressive factor HIO-3, which binds to the Fc domain of huYP218 and pertuzumab, suppresses CD16a Fc- γ receptor activation mediated by huYP218 and pertuzumab via inhibition of the CD16a/IgG Fc interaction. (D) HIO-3 binds to both NAV-003 and huYP218 (red bars); HIO-3 binding to NAV-003, huYP218, or HSA in the presence or absence of soluble competitor proteins (orange bars), wherein x-axis denotes coating protein/soluble competitor. Percentage values next to the bars indicate the percentage of binding reduction in the presence of competitor versus no competitor. * p value < 0.001 versus human serum albumin (HSA). (E) NAV-003 mediates enhanced cytotoxicity against MUC16/CA125 and HIO-3 positive OVCAR3 cells as compared to huYP218. Representative experiments of three independent experiments are shown. Mean values are shown with error bars representing the standard deviations or SEM of sample replica. All statistics were calculated using the unpaired Student's t-test (two-tailed) and the p value is shown within the graph. ns, statistically non-significant.

MUC1 on humoral immune effector activities against tumor cells. The direct binding of the immunosuppressive MUC16/CA125 to IgG1-type antibodies has been shown to suppress immune effector activities and is associated with decreased therapeutic activity in human clinical studies [5–7]. MUC1 has been found to be overexpressed by several carcinomas and its presence has been associated with immunosuppression of ADCC; however, its mechanism of immune effector suppression has not been elucidated [18]. The huYP218 antibody, which constitutes NAV-003's anti-MSLN binding arm, was previously reported to weakly bind MUC16/CA125 [19]. Here, we confirm that NAV-003 poorly binds

to MUC16/CA125 HIO factor (Fig. 4A) while showing unaltered CD16a engagement in the presence of MUC16/CA125 (Fig. 4B). In contrast, the anti-MSLN SS1 antibody, which is bound by MUC16/CA125 (Fig. 4A), shows reduced engagement to the Fc receptor in the presence of MUC16/CA125 (Fig. 4B).

HIO-3 is a member of the intercellular adhesion molecule family and has been recently reported to bind to the CH3 domain of IgG1-type antibodies and inhibit their ADCC [8]. As HIO-3 is present in several MSLN-positive cancers, it could also affect NAV-003 activity. Here, we show that HIO-3 can suppress immune effector activity of pertuzumab and huYP218 by

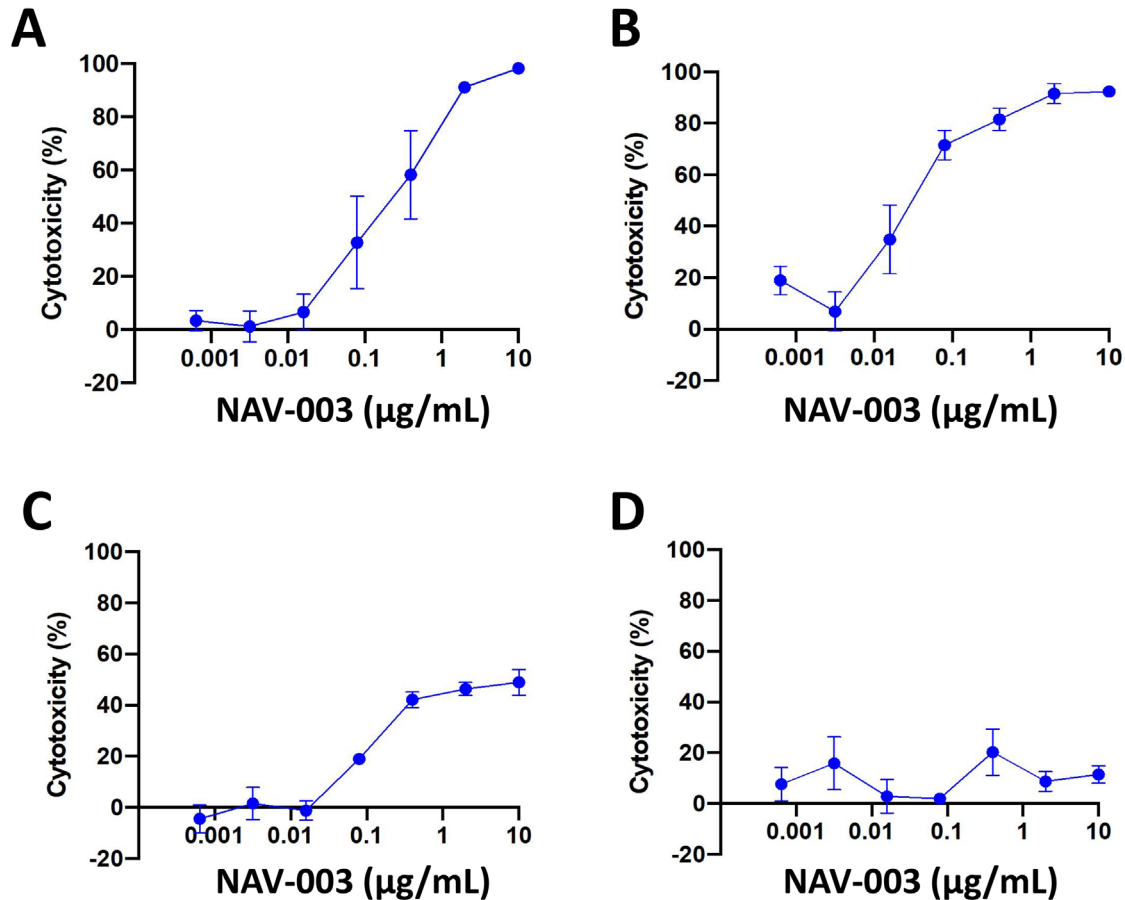


Figure 5. NAV-003 is active against multiple tumor types. NAV-003 shows broad PBMC-mediated cytotoxicity against MSLN-expressing tumor cell lines including OVCAR8 (ovarian, panel A), NCI-Meso63 (mesothelioma, panel B), and KLM-1 (pancreatic, panel C). These effects appear to require MSLN expression as no killing was observed against the isogenic KLM-1-KO where MSLN expression was abolished via CRISPR (panel D). A representative experiment of three independent experiments is shown. Mean values are shown with error bars representing the standard deviations of sample replica.

reducing their engagement and activation of the CD16a/Fc-gamma receptor (Fig. 4C). This effect is mediated by HIO-3 binding to huYP218 antibody as well as NAV-003 (Fig. 4D). A comparative analysis of huYP218- and NAV-003-mediated cytotoxicity on the HIO-3-positive OVCAR3 tumor cells found that NAV-003 was significantly more effective than huYP218, as NAV-003's mode of action relies less on Fc receptor activation, which is affected by HIO-3 and MUC16/CA125, and more on CD3-redirection T-cell-mediated cytotoxicity (Fig. 4E; see also Fig. 3C for NAV-003's EC₅₀ against OVCAR3).

To further determine the potential effects of HIO factors produced by different tumor cell types, including HIO-3 and MUC16/CA125, we evaluated NAV-003 killing activity against other MSLN-positive tumor cell lines in the presence of human PBMCs. The tumor cells tested included OVCAR8 (ovarian cancer), KLM-1 (pancreatic cancer), and NCI-Meso63 (mesothelioma), whose MSLN expression has been previously described [9]. These cell lines express the immunosuppressive factor HIO-3, albeit at different levels, with the NCI-Meso63 tumor, which was used for *in vivo* studies, having the highest expression (Supporting

information Fig. S3). NAV-003 was active against all these lines, with EC₅₀ ranging from 80 to 400 ng/mL (Fig. 5). These effects appeared to require MSLN expression since NAV-003 was inactive at any concentration tested against KLM-1-KO, a MSLN knockout cell line generated via CRISPR [20].

NAV-003 *in vivo* efficacy and tolerability in patient-derived tumor xenografts

As the anti-CD3 ϵ component of NAV-003 does not cross-react with mouse CD3, human PBMCs are needed as effector cells for testing NAV-003's efficacy in mouse models. Optimal adoptive transfer of human PBMCs is a critical aspect to ensure organ colonization and sustained presence of these effector cells for the duration of the experiment. We therefore compared intravenous (IV) and intraperitoneal (IP) routes as the method to transfer human PBMCs into NSG mice. Since the CD4⁺ T-cells subpopulation is an important component supporting a bispecific antibody activity *in vivo* [21, 22], we monitored the presence of human cells in organs

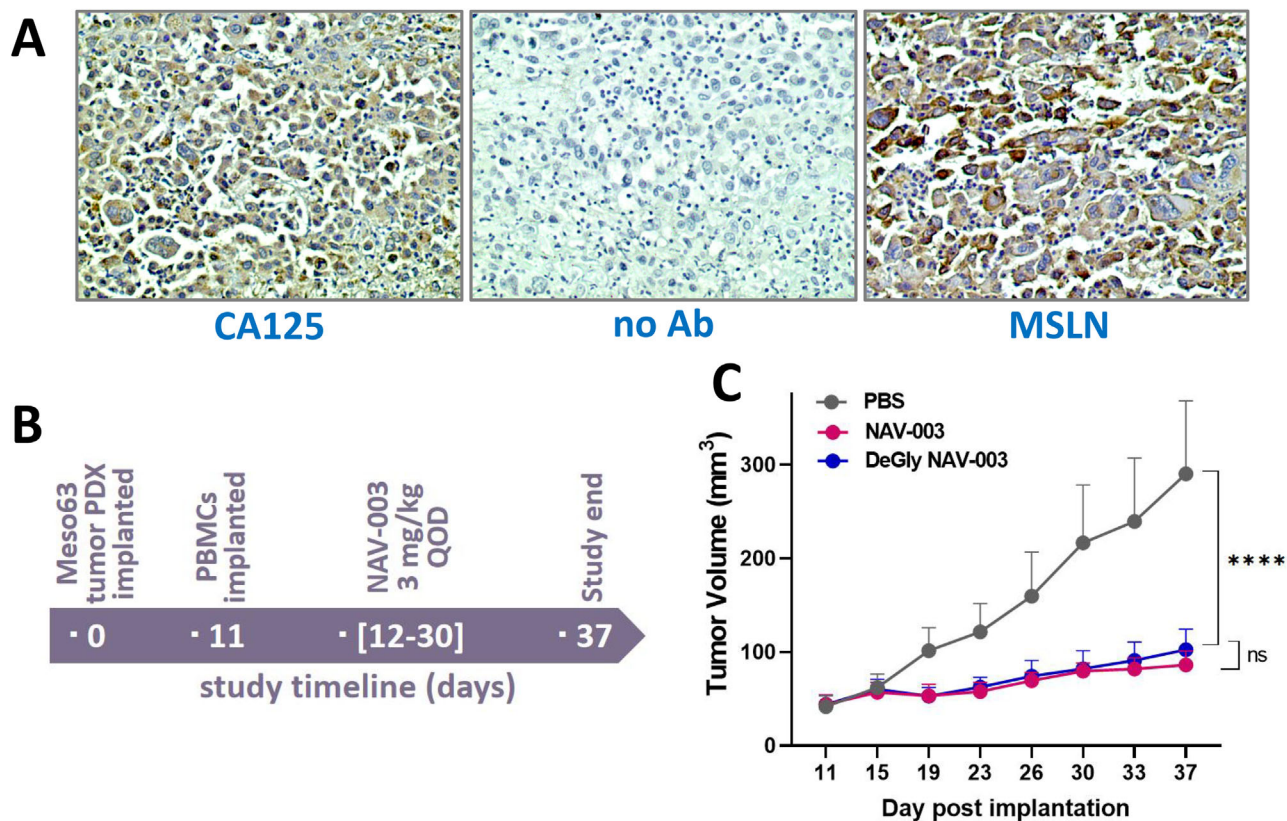


Figure 6. *In vivo* efficacy of NAV-003 in MUC16/CA125 positive mesothelioma PDX. (A) Tumor lesions from NCI-Meso63 PDX were analyzed for MSLN and MUC16/CA125 expression via IHC. Tumors showed robust and homogeneous MSLN and MUC16/CA125 expression. (B) Outline of the human PBMCs adoptive transfer model in NSG mice co-implanted with mesothelioma PDX NCI-Meso63 for NAV-003 efficacy testing. (C) Summary of NAV-003 effect on tumor growth in the NSG model as outlined in panel (B). Both NAV-003 and its deglycosylated form (DeGly NAV-003) showed significant anti-tumor efficacy against NCI-Meso63 tumors. A representative experiment of three independent experiments is shown. Mean values are shown with error bars representing the SEM of six mice per group. All statistics were calculated using the two-way ANOVA with Tukey's multiple comparisons. *****p* value < 0.0001; ns, statistically non-significant.

by using CD4⁺ IHC analysis as well as in circulation by using CD45⁺ FACS analysis. While adoptive transfer of hPBMCs by IV inoculum is a commonly used method, we routinely obtained better colonization when using the IP route for adoptive transfer. Immunohistochemistry analyses at 4-week postadoptive transfer demonstrated a significantly higher number of CD4⁺ cells in the spleen, lung, liver, and lymph nodes when animals were inoculated IP versus IV (Supporting information Fig. S4A and Table S1). In addition, even after 15 days postadoptive transfer, up to 16% of CD45⁺ cells in circulation were still of human origin (Supporting information Fig. S4B).

As previous studies have shown that mesothelioma tumor cells expressing high amounts of HIO factors such as MUC16/CA125 are less responsive to antibody-based agents [5], we sought to test NAV-003 in MSLN-expressing, HIO factor-producing tumor lines. NCI-Meso63 is an early-passaged tumor cell line derived from a patient with pleural mesothelioma and was previously found to express levels of MSLN consistent with those observed in mesothelioma patient tissue [9]. Immunohistochemistry analysis of NCI-Meso63 tumor lesions from untreated xenografts found that both MSLN and MUC16/CA125 had intense, homogeneous

expression, making this tumor cell line an ideal model to test for NAV-003 efficacy (Fig. 6A). Immunodeficient NSG mice were first inoculated subcutaneously with NCI-Meso63 and tumor establishment was monitored until its volume was ≥ 50 mm³. After approximately 11 days, human PBMCs were implanted via IP injection and mice were randomized into groups 24 h later when the treatment was commenced (see study outline in Fig. 6B). Initially, we explored low dose levels (0.4–0.8 mg/kg) since the maximum tolerated dose was not yet known. At the well-tolerated dose level of 0.8 mg/kg, NAV-003 mediated a tumor growth inhibition (TGI) of 32% (Supporting information Fig. S5). Next, tolerability of NAV-003 in NSG mice was further assessed to identify a higher dose level deemed to be well tolerated. The maximum tolerated dose could not be defined since even at the highest dose level tested (3 mg/kg), as well as multiple doses, no significant body weight loss (>10%) or clinical observations were noted (Supporting information Fig. S6). Therefore, in follow up studies we used 3 mg/kg of NAV-003 or DeGly NAV-003 administered every other day for 3 weeks. As shown in Fig. 6C, both NAV-003 and DeGly NAV-003 treatments resulted in significant suppression of tumor growth (70%) as compared to PBS control

($p < 0.0001$). Overall, NAV-003-mediated anti-tumor response appeared to be dose-dependent (32% TGI at 0.8 mg/kg vs. 70% TGI at 3 mg/kg). As there were no significant differences in TGI between NAV-003 and DeGly NAV-003 treatments, and contrary to previously published observations [15], loss of Fc receptor binding did not improve or worsen the anti-tumor effects mediated by NAV-003. In total, these data demonstrate that NAV-003 has good potency across a spectrum of MSLN-expressing tumor lines *in vitro*, is refractory to HIO factors producing tumor cells, and is effective against patient-derived mesothelioma *in vivo*.

Discussion

We have adopted a bispecific antibody approach to develop NAV-003, an optimized targeting agent that can effectively kill immunosuppressed MSLN-positive cancers. The steps taken to achieve this optimization included configuring the bispecific format on a fully humanized anti-MSLN IgG1 antibody backbone, employing a high-affinity tumor-targeting anti-MSLN antibody (huYP218) that binds to a unique epitope located within the proximal cell surface region III of the MSLN protein, and genetically fusing an anti-CD3 ϵ single-chain antibody to the huYP218 N-terminal light chain via optimized spacer length to maximize tumor-lymphocyte juxtapositioning for tumor-specific activation and efficient tumor cell killing. Analysis of NAV-003 has shown that it is effective in killing MSLN-expressing tumor cells mainly via its CD3-redirected, T-cell-mediated cytotoxicity. Moreover, here we report that the use of full-length IgG-bispecific antibody can enhance target cell killing in the presence of immunosuppressive tumor-produced HIO factors previously shown to have a negative impact on antibodies whose mode of action is mediated by ADCC and CDC immune effector killing [5-8, 17, 18]. We also investigated the impact of Fc receptor binding, or lack thereof, on NAV-003 activity *in vivo*. The NSG strain used in our studies can be affected by altered *in vivo* distribution of humanized IgG1 antibody (same as NAV-003) with possible accumulation in nontarget organs such as the spleen and bones. This tissue sequestration is mediated by the Fc receptor expressed in certain cell subtypes and was elegantly demonstrated by Sharma et al. [23]. Although this phenomenon appeared to reduce the effectiveness of other bispecific constructs [15], it did not alter the efficacy of NAV-003, also supporting the results *in vitro* where the cytotoxicity component mediated through the Fc- γ receptor is less prominent when compared to the CD3-redirected, T-cell-mediated cytotoxicity (Fig. 3C).

While much effort has been employed by the industry to improve upon bispecific antibody therapeutics such as antibody configuration, antibody valency for tumor and immune cell antigens, and spacing of antigen binding domains, other factors including epitope positioning as well as optimized ADCC and CD8⁺ T-cell activation of cytotoxic modalities are just some of the other challenges thought to empirically affect the development of potent bispecific antibodies [24]. A recent study by Hatterer described a similar aspect where the targeting of MSLN region

III enhanced cytotoxicity compared to membrane-distal domains when bispecific formats were used [25]. MSLN-positive cancers are well known to co-express immunosuppressive HIO factors. Cancers expressing high MSLN levels such as malignant pleural mesothelioma, nonmucinous ovarian, endometrial, and pancreatic adenocarcinoma have all been documented to express the immunosuppressive MUC16/CA125 [26-28] as well as MUC1 [29-32]. Antibody-based therapies that employ ADCC and CDC immune effector activities have had modest efficacy in treating these diseases and only few studies have correlated HIO factor levels with preclinical or clinical outcomes. Amatuximab, also known as MORAb-009, which incorporates the SS1 variable domain, is one of the most clinically investigated antibodies targeting MSLN-positive cancers. Amatuximab has been tested in Phase 2 clinical trials in patients with stage III/IV primary unresectable malignant pleural mesothelioma (clinical trial NCT00738582) [33] and in first-line stage III/IV pancreatic adenocarcinoma (clinical trial NCT00570713) [34], which are two cancer indications in which the MUC16/CA125 HIO factor is highly expressed. While no statistical difference in tumor response was observed in the pancreatic cancer study, an improvement over historical responses was observed in the mesothelioma trial. Interestingly, a *post hoc* analysis showed a 2- and 7-month improvement in progression-free survival (PFS) (HR 0.43, $p = 0.0062$) and overall survival (OS) (HR 0.40, $p = 0.0022$) in patients that had low levels of the MUC16/CA125 as compared to those with high levels [5]. These data were similar to those found in an ovarian cancer Phase 3 trial comparing the experimental farletuzumab antibody, whose mechanism of action is ADCC and CDC, where patients with low levels of MUC16/CA125 had a statistically significant improvement in PFS (HR 0.49, $p = 0.0028$) and OS (HR 0.44, $p = 0.0108$) as compared to those with high levels [35]. Interestingly, analysis of the placebo control arm that consisted of 357 patients found that MUC16/CA125 levels had no difference in PFS or OS, suggesting a direct correlation with farletuzumab therapeutic activity, which was subsequently confirmed experimentally [7]. Similar data have been reported for MUC1 and the trastuzumab antibody where clinical resistance to therapy in breast cancer is associated with overexpression of MUC1 and can be reversed using MUC1 antagonists [36]. These data suggest that antibody-based therapies can be negatively affected by HIO factors and that alternative formats such as optimized bispecific antibodies may be more effective in cancers producing high levels of these factors.

Materials and methods

Proteins, antibodies, and bispecific antibody

Immunosuppressive MUC16/CA125 HIO factor was purchased from Lee Biosystems. The immunosuppressive HIO-3 factor was produced recombinantly as a poly-histidine tagged fusion protein and purified via nickel column chromatography. Antibodies were either purchased from vendors or obtained through academic

collaboration. Analytical antibodies including anti-IL2-HRP (Sino Biological), anti-CD4 (Novus), anti-human CD45 (BioLegend), anti-human CD45 (BioLegend), humanized SS1 (Creative Bio-Labs), and pertuzumab (MedChemExpress) were purchased from vendors. Rabbit YP218 and huYP218 were obtained from Dr. Mitchell Ho at the National Cancer Institute (Bethesda, MD) and are characterized as previously described [10]. Humanized anti-CD3 ϵ (huOKT3) was generated from parent OKT3 antibody by grafting parent variable sequences onto a human IgG1 backbone. The NAV-003 bispecific antibody was made by engineering a construct containing a cDNA encoding for the humanized anti-CD3 ϵ , formatted as a single chain antibody (scFv), with an optimized GGGGS(x) repeat linker between light and heavy chain CDRs. The anti-CD3 ϵ scFv was cloned upstream of the mature N-terminal domain of the huYP218 light chain via an optimized linker encoding the amino acids GGGGS(x). The anti-CD3/huYP218 light chain and huYP218 heavy chain cDNAs were cloned into the pXC vector (Lonza) that has two CMV driven expression cassettes and the glutamine synthase (GS) selection gene cassette to create pNAV-003 plasmid. To generate stable recombinant production cell lines, CHOK1SV-GSKO cells containing a knocked-out GS locus were cultured at 6.0×10^5 cell/mL in CD-CHO (Irving Scientific) plus 6 mM L-glutamine overnight at 37°C in 5% CO₂. The next day, 2.0×10^7 cells were resuspended with 20 μ g of pNAV-003 expression plasmid in a total volume of 700 μ L plain CD-CHO, then transferred to a 0.4 cm electroporation cuvette and electroporated at 300 V/900 μ F using the BioRad GenePulser II. Cells were incubated overnight at 37°C in 5% CO₂ in CD-CHO plus 6 mM L-glutamine in a shaking platform incubator. The following day, cells were reseeded in CD-CHO/SP4 medium containing 50 μ M MSX (Sigma) for GS selection. After selection, pools were subcloned by limiting dilution and conditioned media were tested for recombinant NAV-003 antibody concentrations via ELISA using an anti-human IgG1 capture and anti-human Fc-HRP probe as described below. The best production clones were expanded for NAV-003 isolation via protein A chromatography as previously described [6] and analyzed for homogeneity via SDS-PAGE and antigen binding via ELISA and/or immunofluorescent cell staining as described below. To generate deglycosylated NAV-003 (DeGly NAV-003), 10 mg of NAV-003 was deglycosylated enzymatically using *GlycINA-TOR MidiSpin* column following the manufacturer's instructions (Genovis Inc., Cambridge, MA). After treatment, DeGly NAV-003 preparations were analyzed by SDS-PAGE to monitor shift in molecular weight as compared to native NAV-003 as well as CD16a Fc receptor and C1q protein binding as described below. Multiple high-quality preparations were then tested for efficacy against various tumor cell lines *in vitro* and *in vivo*.

Surface plasmon resonance analyses

The carboxymethylated dextran surface of the CM5 sensor chips (Cytiva) were used to carry out affinity analyses by using a Biacore instrument (T200). After activation, NAV-003 (5 μ g/mL) was

immobilized on the chip until the desired response units were achieved (~160 RU). The recombinant human CD3E & CD3G dimer (CD3) and human MSLN (Sino Biological) were diluted in running buffer (10 mM HEPES, 150 mM NaCl, 0.05% Tween-20, pH 7.4) at the concentrations shown in the figures. Then, CD3 and MSLN were injected in separate channels and flowed over the immobilized NAV-003 at a constant flow rate of 30 μ L/min at 25°C. The antigen-antibody interaction was observed for 90 s of association followed by 300 s of dissociation. The residual ligands were removed by washing the chip with 10 mM glycine (pH 1.5) for 30 s at 30 μ L/min. For co-binding, MSLN was flowed over first and CD3 was flowed next using similar conditions as above. The BIA evaluation 4.1 software was used to estimate the KD values. Three independent measurements were performed.

Cell lines, PBMCs, and patient-derived cell line

The human ovarian cancer OVCAR3, Chinese Hamster Ovary (CHO), and T-cell lymphoma Jurkat cells were purchased from ATCC and maintained in complete RPMI1640 medium (R7.5) containing 7.5% fetal bovine serum (FBS), 2 mM L-glutamine, and 100 U penicillin-streptomycin. Recombinant CHO cells stably expressing human MSLN (CHO-MSLN) were generated using Lipofectamine 3000 (ThermoFisher Scientific, Waltham, MA) and maintained in R7.5 plus zeocin selection media. Tumor cell lines OVCAR8, KLM-1, and KLM-1-KO were maintained in complete RPMI1640 medium (R10) containing 10% FBS, 2 mM L-glutamine, and 100 U penicillin-streptomycin while early-passage patient-derived NCI-Meso63 cells [9] were cultured in RPMI1640 medium (R20) containing 20% FBS, 2 mM L-glutamine, 100 U penicillin-streptomycin, and 1 mM sodium pyruvate (Invitrogen, CA). NCI-Meso63 (RH63) was established from pleural fluid obtained from a mesothelioma patient under the Institutional Review Board (IRB)-approved protocol (ClinicalTrials.gov NCT 01950572). PBMCs from healthy donors were obtained from the NIH Clinical Center Department of Transfusion Medicine under their IRB approved and consented healthy donor program or purified by Ficoll separation from commercial leukopacks (BioIVT, Hicksville, NY). All studies were conducted in accordance with the Declaration of Helsinki, and informed written consent was obtained from each subject.

Cytotoxicity assays

To test for antibody-mediated killing activity of target cell lines, $2-10 \times 10^3$ target cells were plated in opaque (for CellTiter-Glo® analysis) or clear 96-well plates overnight in appropriate growth media. The next day, various concentrations of antibody plus IL-2-stimulated PBMCs were added to each well at an effector:target ratio varying from 10:1 to 40:1. Plates were incubated at 37°C in 5% CO₂ for 96 h. Wells were then washed three times with Dulbecco's phosphate saline buffer without Mg⁺⁺ or Ca⁺⁺ (DPBS) to remove PBMCs and the adherent target cell viability

was quantified by CellTiter-Glo® as per manufacturer's directions (Promega) or by crystal violet staining. For crystal violet staining, plates were washed three times with DPBS, stained for 10 min, washed in distilled water five times, air dried, solubilized in 1% SDS, and quantified on a Varioskan plate reader at 570 nm.

Jurkat CD16a-luciferase activation and Jurkat IL-2 stimulation assays

The Jurkat CD16a-luciferase reporter cell line (Promega) was employed to monitor CD16a Fc-gamma receptor activation of various antibodies in the presence or absence of HIO factors as well as various target cell lines. Briefly, 2.5×10^3 target cells were plated into opaque 96-well plates in appropriate growth media and incubated for 48 h at 37°C in 5% CO₂. Wells were then replated in phenol-red free RPMI1640 medium (R1, containing 1% FBS, 2 mM L-glutamine, and 100 U penicillin-streptomycin), 0.5×10^6 Jurkat-CD16a-luciferase cells with 0.1–5 µg/mL antibody treatments, and varying amounts of HIO factors in triplicates. Cultures were grown 12–18 h at 37°C in 5% CO₂ and then analyzed for CD16a Fc-gamma receptor activation using the Bio-Glo™ luciferase assay following the manufacturer's instructions (Promega). Plates were quantified on a luminescent Varioskan plate reader and values represented as relative light units (RLU).

For Jurkat IL-2 production assays, clear 96-well plates were seeded with or without 2.5×10^3 CHO or CHO-MSLN target cells in R7.5 growth media and incubated for 48 h at 37°C in 5% CO₂. Wells were then replated with R7.5 growth medium and 0.5×10^6 parent Jurkat cells with media only, 2.5 µg/mL NAV-003, or huYP218 antibody in triplicates for 24 h at 37°C in 5% CO₂. Plates were centrifuged and culture supernatants isolated and stored at –20°C.

ELISA and immunofluorescence cell staining

ELISA and immunofluorescent cell staining assays were used to measure MSLN, CD3ε, IL-2, and human serum albumin (HSA, negative control) binding of antibodies as previously described [5, 6]. Briefly, for testing of anti-MSLN and anti-CD3ε binding, clear 96-well plates were coated with 100 ng/mL of recombinant MSLN (Sino Biological), CD3ε (Sino Biological), or 100 ng/mL of HSA (Sigma) in 0.05 M carbonate buffer, pH 9.5 overnight at 4°C. For IL-2 analysis of parent Jurkat culture supernatants, clear 96-well plates were coated with supernatants diluted 1:2, 25–0.05 ng/mL recombinant human IL-2 (Sino Biological) or 100 ng/mL of HSA in carbonate buffer overnight at 4°C. Next, plates were washed with 0.05 M phosphate buffer, pH 7.2 (PB) and blocked in PB plus 5% bovine serum albumin (BSA) for 1 h at room temperature. For anti-MSLN and anti-CD3ε binding, wells were washed with PB then probed with 2.5 µg/mL of biotinylated humanized SS1, huYP218, humanized OKT3 (huOKT3), or NAV-003 antibody in PB plus 0.5% BSA for 1 h at room temperature. For anti-IL2 assays, plates were washed and probed with 0.5 µg/mL rab-

bit anti-huIL2-HRP in PB plus 0.5% BSA for 1 h. After primary probing, wells were washed with PB and secondary probed with 333 ng/mL streptavidin-horse radish peroxidase (HRP) (Jackson ImmunoResearch Laboratories), or for IL-2 ELISAs, plates washed with PB, then incubated with TMB substrate for 10–30 min. Reactions were stopped with 0.1 N H₂SO₄ and plates were analyzed for absorbance at 450 nm using a Varioskan plate reader. For quantitation, standard curves were analyzed in Prism 9.5 by interpolation of XY: dose versus response (sigmoidal nonlinear regression).

For immunofluorescent cell staining, 1.0×10^6 CD3⁺/MSLN[–] parental Jurkat cells were stained with 1 µg/mL of biotinylated NAV-003, huYP218 or huOKT3 for 1 h on ice, washed in DPBS and stained with 0.5 µg/mL of streptavidin-AF488 secondary antibody (Thermo Scientific). Cells were washed with DPBS then analyzed for antibody binding via fluorescence and total cell counts using a Countess cell analyzer following the manufacturer's instructions (Thermo Scientific). Antibodies were biotinylated using sulfo-tag conjugation (Meso Scale Diagnostics) as previously described with multiple independent lots generated to confirm reproducibility [5].

CD16a/Fc-γ receptor and C1q binding assay

Clear 96-well ELISA plates were coated with 2.5 µg/mL native or deglycosylated NAV-003 in 50 mM carbonate buffer, pH 9.5 overnight at 4°C. The following day, plates were aspirated and wells blocked with PB plus 5% BSA (ELISA assay buffer) for 1 h at room temperature. Plates were washed with PB and then probed with 1 µg/mL biotinylated CD16a or C1q in ELISA assay buffer with shaking for 1 h. Next, plates were washed three times with PB, probed with 333 ng/mL streptavidin-HRP secondary antibody in ELISA assay buffer, and incubated for 1 h at room temperature with shaking. Finally, wells were washed five times with PB and developed with addition of TMB substrate for 5–30 min at room temperature. Reactions were stopped with 0.1 N H₂SO₄ and plates were analyzed for absorbance at 450 nm using a Varioskan plate reader.

HIO-3 binding assay and competition

ELISA plate was coated for 1 h at room temperature with 50 µL of 2 µg/mL NAV-003, huYP218, or HSA in carbonate coating buffer. Wells were aspirated and blocked for 1 h at room temperature with 100 µL Pierce Block solution. Wells were aspirated and 50 µL of 10 µg/mL soluble competitors were added in ELISA assay buffer (A.B., PBS + 1% BSA). Biotinylated HIO-3 (b-HIO-3) was added at a final concentration of 1.5 µg/mL. Plate was washed at room temperature for 1 h. After three washes with PBS/Tween (PBS-T), 100 µL of 50 ng/mL streptavidin-HRP in A.B. was added and incubated for 1 h. After washes with PBS-T, 75 µL of TMB substrate was added for 5 min at room temperature followed by addition of an equal volume of 0.1 N H₂SO₄ to stop the reaction. Binding of b-HIO3 was quantitated by reading absorbance at

450 nm. Competitive binding of b-HIO3 by soluble antibodies was quantitated by comparing the signal obtained by b-HIO-3 binding to NAV-003 coated wells without competitor.

HIO-3 expression analysis

Cells were washed with PBS, and then lysed with RIPA buffer at 1×10^7 cell/mL. Insoluble material was pelleted and the lysates were transferred to fresh tubes. Lysates (75 μ L) were mixed with 25 μ L 4 \times Laemmli loading buffer containing 2-mercaptoethanol. Samples were heated at 95°C for 5 min and then 10 μ L loaded on duplicate 4–12% bis-Tris polyacrylamide gels and electrophoresed at 180 V for 35 min. Gels were electroblotted onto PVDF membranes for 1 h at 30 V. After 1-h blocking in 5% milk/PBST, one blot was probed with a 1:1000 dilution of rabbit polyclonal anti-HIO-3 antibody. As a loading control, the second blot was probed with a 1:2500 dilution of polyclonal rabbit anti-GAPDH (Abcam), both for 1 h at room temperature. After three washes with PBS-T, both blots were probed with a 1:5000 dilution of goat anti-rabbit-HRP for 1 h, washed again, and then exposed to ECL substrate (Pierce) for band visualization.

IHC and FACS analysis

To confirm MSLN and MUC16/CA125 expression in NCI-Meso63 tumors, as well as human CD4 expression in human effector cells colonized mouse organs, we employed IHC using a rabbit anti-MSLN antibody that binds to the same epitope as NAV-003, a rabbit anti-CA125 antibody (Novus), and a rabbit anti-human CD4 antibody (Novus), respectively. Briefly, 5 μ m sections of paraffin embedded tumor fragments were sectioned then adhered to glass slides. Sections were deparaffinized and prepared for antigen retrieval in boiling 10 mM sodium citrate, pH 6.0 for 10 min, then equilibrated with phosphate buffered saline-0.05% tween-20 (PBS-T). Sections were quenched for endogenous peroxidase activity using 0.3% peroxidase/methanol for 10 min and blocked for 1 h in 10% goat serum in PBS-T. Next, slides were rinsed in PBS-T and probed for MSLN, MUC16/CA125, or CD4 using 3 μ g/mL of each primary antibody diluted in blocking buffer for 1.5 h followed by PBS-T washing, secondary blocking for 1 h, and probing with 5 μ g/mL of an anti-rabbit-HRP conjugated antibody for 1 h. Control slides were incubated with no primary antibody. Slides were then washed in PBS-T and developed using eBioscience DAB advanced chromogenic substrate as recommended by the manufacturer (Thermo Scientific). Finally, samples were hematoxylin counterstained, cover-slipped, and analyzed for antigen expression under light microscopy. Membranous staining was considered positive.

FACS analysis was conducted on blood cells from mice administered with human PBMCs via IP route. Whole blood was collected and analyzed for mouse and human CD45⁺ cells as previously described [9]. Briefly, the whole blood was stained with fluorescent dye-conjugated antibodies. Ammonium-chloride-

potassium lysing buffer was used for the lysis of red blood cells before the samples were analyzed by flow cytometry. All flow cytometry detection was performed on CytoFLEX LX and analyzed using FlowJo software.

In vivo efficacy models using patient-derived mesothelioma cancer cells

Eighteen 5- to 6-week-old female NSG mice were inoculated with 8.0×10^6 patient-derived NCI-Meso63 tumor cells [9] subcutaneously and tumor growth was monitored for 10 days. Mice with established tumors (40–100 mm³) were then randomized and administered 1.0×10^7 PBMCs intraperitoneally. After 24 h, mice were randomized into three treatment groups (N = 6 per group) and administered PBS or 3 mg/kg of NAV-003 or DeGly NAV-003 antibody intravenously every other day for 3 weeks. Body weights and tumor volumes (mm³) were carried out by caliper measurement twice weekly. Termination of mice was carried out at the set study termination period of day 37 postrandomization.

Statistics

P values for data generated by ELISA and *in vitro* cell killing or activation assays were calculated using the Student's *t*-test. All other *p* values were calculated via one- or two-way ANOVA, with Dunnett's or Tukey's multiple comparisons test using Prism 9.5 software. Results were considered to be significant if *p* < 0.05.

Acknowledgements: R.H. and Q.J. were supported by the Intramural Research Program of the NIH, National Cancer Institute, Center for Cancer Research (ZIA-BC-010816). Remaining work was funded by Navrogen Inc.

Conflict of interest: The authors declare no commercial or financial conflict of interest.

Ethics approval: All animal studies were approved by Animal Care and Use Committee of the NCI, NIH (Bethesda, MD). NOD.scid gamma (NSG) mice were obtained from the Jackson Laboratory. All mice were maintained in a dedicated pathogen-free environment following NIH guidelines approved by the NCI Animal Care and Use Committee. All *in vivo* experimental efforts were made to minimize animal suffering and monitored by licensed veterinarians.

Data availability statement: The data that support the findings of this study are available from the corresponding author upon reasonable request.

Peer review: The peer review history for this article is available at <https://publons.com/publon/10.1002/eji.202250309>

References

- Hassan, R., Thomas, A., Alewine, C., Le, D. T., Jaffee, E. M. and Pastan, I., Mesothelin immunotherapy for cancer: ready for prime time? *J. Clin. Oncol.* 2016. **34**: 4171–4179.
- Rump, A., Morikawa, Y., Tanaka, M., Minami, S., Umesaki, N., Takeuchi, M. and Miyajima, A., Binding of ovarian cancer antigen CA125/MUC16 to mesothelin mediates cell adhesion. *J. Biol. Chem.* 2004. **279**: 9190–9198.
- Hassan, R., Ebel, W., Routhier, E. L., Patel, R., Kline, J. B., Zhang, J., Chao, Q. et al. Preclinical evaluation of MORAb-009, a chimeric antibody targeting tumor-associated mesothelin. *Cancer Immunol.* 2007. **7**:20–30.
- Pastan, I. and Hassan, R. Discovery of mesothelin and exploiting it as a target for immunotherapy. *Cancer Res.* 2014. **74**: 2907–2912.
- Nicolaides, N. C., Schweizer, C., Wang, W., Somers, E. B., Ross, E. N., Fernando, S., Grasso, L. et al. CA125 suppresses immune-effector function of amatuximab and elevated levels are associated with reduced amatuximab clinical response in first line mesothelioma patients. *Cancer Biol Ther.* 2018. **19**:622–630.
- Grasso, L., Kline, J. B. and Nicolaides, N. C. Block-Removed Immunoglobulin Technology (BRITE) to enhance rituximab effector function by counteracting CA125-mediated immunosuppression. *Oncol Lett.* 2022. **23**:2–12.
- Kline, J. B., Kennedy, R. P., Albone, E., Chao, Q., Fernando, S., McDonough, J. M., Rybinski, K. et al. Tumor antigen CA125 suppresses antibody-dependent cellular cytotoxicity (ADCC) via direct antibody binding and suppressed Fc receptor engagement. *OncoTarget.* 2017. **8**:52045–52060.
- Kline, J. B., Grasso, L. and Nicolaides, N. C. Discovery of HIO-3, a tumor-produced protein that binds the human IgG1 Fc CH3 domain and suppresses antibody-dependent cellular cytotoxicity (ADCC) and complement-dependent cytotoxicity (CDC). *J. Immunother. Cancer.* 2022. **10**. <https://doi.org/10.1136/jitc-2022-SITC2022.1432>
- Tomar, S., Zhang, J., Khanal, M., Hong, J., Venugopalan, A., Jiang, Q., Sengupta, M. et al. Development of highly effective anti-mesothelin hYP218 chimeric antigen receptor T cells with increased tumor infiltration and persistence for treating solid tumors. *Mol. Cancer Ther.* 2022. **21**:1195–1206.
- Zhang, Y. F., Phung, Y., Gao, W., Kawa, S., Hassan, R., Pastan, I. and Ho, M. New high affinity monoclonal antibodies recognize non-overlapping epitopes on mesothelin for monitoring and treating mesothelioma. *Sci Rep.* 2015. **21**:1–14.
- Jiang, Q., Ghafoor, A., Mian, I., Rathkey, D., Thomas, A., Alewine, C., Sengupta, M. et al. Enhanced efficacy of mesothelin-targeted immunotoxin LMB-100 and anti-PD-1 antibody in patients with mesothelioma and mouse tumor models. *Sci Transl Med.* 2020. **12**(550): eaz7252.
- Santich, B. H., Park, J. A., Tran, H., Guo, H. F., Huse, M. and Cheung, N. K. V. Interdomain spacing and spatial configuration drive the potency of IgG-[L]-ScFv T-cell bispecific antibodies. *Sci Transl Med.* 2020. **12**:1–26.
- Compte, M., Alvarez-Cienfuegos, A., Nuñez-Prado, N., Sainz-Pastor, N., Blanco-Toribio, A., Pescador, N., Sanz, L. et al. Functional comparison of single-chain and two-chain anti-CD3-based bispecific antibodies in gene immunotherapy applications. *Oncoimmunology.* 2014. **3**: e28810.
- Mandikian, D., Takahashi, N., Lo, A. A., Li, J., Eastham-Anderson, J., Slaga, D., Ho, J. et al. Relative target affinities of T-cell-dependent bispecific antibodies determine biodistribution in a solid tumor mouse model. *Mol. Cancer Ther.* 2018. **17**: 776–785.
- Wang, L., Hoseini, S. S., Xu, H., Ponomarev, V. and Cheung, N. K. Silencing Fc domains in T cell-engaging bispecific antibodies improves T-cell trafficking and antitumor potency. *Cancer Immunol Res.* 2019. **7**:2013–2024.
- Fraser, C. C., Jia, B., Hu, G., Ibrahim, L., Johani, A., Fritz-Klaus, R. et al. Ovarian cancer ascites inhibits transcriptional activation of NK cells partly through CA125. *J. Immunol.* 2022. **208**:2227–2238.
- Zhang, K., Sikut, R. and Hansson, G. C. A MUC1 mucin secreted from a colon carcinoma cell line inhibits target cell lysis by natural killer cells. *Cell Immunol.* 1997. **176**:158–165.
- Moreno, M., Bontkes, H. J., Scheper, R. J., Kenemans, P., Verheijen, R. H. M. and von Mensdorff-Pouilly, S. High level of MUC1 in serum of ovarian and breast cancer patients inhibits huHMFG-1 dependent cell-mediated cytotoxicity (ADCC). *Cancer Lett.* 2007. **257**:47–55.
- Nicolaides, N. C., Kline, J. B. and Grasso, L. NAV-001, a high-efficacy antibody-drug conjugate targeting mesothelin with improved delivery of a potent payload by counteracting MUC16/CA125 inhibitory effects. *PLoS One.* 2023. **18**(5):e0285161.
- Avula, L. R., Rudloff, M., El-Behaedi, S., Arons, D., Albalawy, R., Chen, X., Zhang, X. et al. Mesothelin enhances tumor vascularity in newly forming pancreatic peritoneal metastases. *Mol. Cancer Res.* 2020. **18**: 229–239.
- Haas, C., Krinner, E., Brischwein, K., Hoffmann, P., Lutterbüse, R., Schlereth, B., Kufer, P. et al. Mode of cytotoxic action of T cell-engaging BiTE antibody MT110. *Immunobiology.* 2009. **214**(6):441–453.
- Feldmann, A., Arndt, C., Töpfer, K., Stamova, S., Krone, F., Cartellieri, M., Koristka, S. et al. Novel humanized and highly efficient bispecific antibodies mediate killing of prostate stem cell antigen-expressing tumor cells by CD8+ and CD4+ T cells. *J. Immunol.* 2012. **189**(6):3249–3259.
- Sharma, S. K., Chow, A., Monette, S., Vivier, D., Pourat, J., Edwards, K. J., Dilling, T. R. et al. Fc-mediated anomalous biodistribution of therapeutic antibodies in immunodeficient mouse models. *Cancer Res.* 2018. **78**(7):1820–1832.
- Brinkmann, U. and Kontermann, R. E. The making of bispecific antibodies. *MAbs.* 2017. **9**(2):182–212.
- Hatterer, E., Chauchet, X., Richard, F., Barba, L., Moine, V. et al. Targeting a membrane-proximal epitope on mesothelin increases the tumoricidal activity of a bispecific antibody blocking CD47 on mesothelin-positive tumors. *MABS.* 2020. **12**:1–13.
- Kaneko, O., Gong, L., Zhang, J., Hansen, J. K., Hassan, R., Lee, B. and Ho, M. A binding domain on mesothelin for CA125/MUC16. *Protein Struct. Fold.* 2009. **284**:3739–3749.
- Kakimoto, S., Miyamoto, M., Einama, T., Takihata, Y., Matsuura, H. et al. Significance of mesothelin and CA125 expression in endometrial carcinoma: a retrospective analysis. *Diagnost. Pathol.* 2021. **16**:1–10.
- Takahiro, K., Hirofumi, N., Hiroshi, H., Shigenori, K., Hiromi, T. et al. Co-expression of mesothelin and CA125 correlates with unfavorable patient outcome in pancreatic ductal adenocarcinoma. *Pancreas.* 2011. **40**:1276–1282.
- Creaney, J., Segal, A., Sterrett, G., Platten, M. A., Baker, E. et al. Overexpression and altered glycosylation of MUC1 in malignant mesothelioma. *Br J Cancer.* 2008. **98**:1562–1569.
- Qu, C. F., Li, Y., Song, Y. J., Rizvi, S. M. A., Raja, C., Zhang, D., Samra, J. et al. MUC1 expression in primary and metastatic pancreatic cancer cells for in vitro treatment by 213Bi-C595 radioimmunoconjugate. *Br J Cancer.* 2004. **91**:2086–2093.

- 31 Wang, L., Ma, J., Liu, F., Yu, Q., Chu, G., Perkins, A. C. and Li, Y. Expression of MUC1 in primary and metastatic human epithelial ovarian cancer and its therapeutic significance. *Gynecol Oncol* 2007. **105**:695–702.
- 32 Morrison, C., Merati, K., Marsh, W. L. Jr., De Lott, L., Cohn, D. E., Young, G. and Frankel, W. L. The mucin expression profile of endometrial carcinoma and correlation with clinical-pathologic parameters. *Appl Immunohistochem Mol Morphol* 2007. **15**:426–431.
- 33 Hassan, R., Kindler, H. L., Jahan, T., Bazhenova, L., Reck, M., Thomas, A., Pastan, I. et al. Phase II clinical trial of amatuximab, a chimeric anti-mesothelin antibody with pemetrexed and cisplatin in advanced unresectable pleural mesothelioma. *Clin Cancer Res* 2014. **20**:5927–5936.
- 34 Pastan, I. and Hassan, R. Discovery of mesothelin and exploiting it as a target for immunotherapy. *Cancer Res* 2014. **74**:2907–2912.
- 35 Vergote, I., Armstrong, D., Scambia, G., Teneriello, M., Sehouli, J., Weil, S. C. et al. A randomized, double-blind, placebo-controlled, phase III study to assess efficacy and safety of weekly farletuzumab in combination with carboplatin and taxane in patients with ovarian cancer in first platinum-sensitive relapse. *J Clin Oncol* 2016. **34**:2271–2278.
- 36 Namba, M., Hattori, N., Hamada, H., Yamaguchi, K., Okamoto, Y., Nakashima, T., Masuda, T. et al. Anti-KL- 6/MUC1 monoclonal antibody

reverses resistance to trastuzumab-mediated antibody-dependent cell-mediated cytotoxicity by capping MUC1. *Cancer Lett* 2019. **442**:31–39.

Abbreviations: HIO: humoral immune-oncology · MSLN: mesothelin · ADCC: antibody dependent cellular cytotoxicity · CDC: complement dependent cytotoxicity · FBS: fetal bovine serum · GS: glutamine synthase · HRP: horse radish peroxidase · HSA: human serum albumin · TGI: tumor growth inhibition

Full correspondence: Dr. Luigi Grasso, Navrogen Inc., 1837 University Circle, Cheyney, PA 19319, USA
e-mail: luigi@navrogen.com

Received: 5/12/2022

Revised: 3/5/2023

Accepted: 4/5/2023

Accepted article online: 5/5/2023